Higgs-strahlung and Vector Boson Fusion in e^+e^- Collisions

W. Kilian, M. Krämer, and P.M. Zerwas
Deutsches Elektronen-Synchrotron DESY, D-22603 Hamburg/FRG

Abstract

Higgs-strahlung $e^+e^- \to ZH$ and WW (ZZ) fusion $e^+e^- \to \bar{\nu}_e\nu_e H$ (e^+e^-H) are the most important mechanisms for the production of Higgs bosons at future e^+e^- linear colliders. We have calculated the cross sections and energy/angular distributions of the Higgs boson for these production mechanisms. When the Z boson decays into (electron-)neutrinos or e^+e^-, the two production amplitudes interfere. In the cross-over region between the two mechanisms the interference term is positive (negative) for $\bar{\nu}_e\nu_e$ (e^+e^-) decays, respectively, thus enhancing (reducing) the production rate.

1. The analysis of the mechanism which breaks the electroweak gauge symmetry $SU(2)_{\rm L} \times U(1)_{\rm Y}$ down to $U(1)_{\rm EM}$, is one of the key problems in particle physics. If the gauge fields involved remain weakly interacting up to high energies – a prerequisite for the (perturbative) renormalization of $\sin^2\theta_W$ from the symmetry value 3/8 of grand-unified theories down to a value near 0.2 at low energies – fundamental scalar Higgs bosons [1] must exist which damp the rise of the scattering amplitudes of massive gauge particles at high energies. In the Standard Model (SM) an isoscalar doublet field is introduced to accomodate the electroweak data, leading to the prediction of a single Higgs boson. Supersymmetric extensions of the Standard Model expand the scalar sector to a spectrum of Higgs particles [2]. The Higgs particles have been searched for, unsuccessfully so far, at LEP1, setting a lower limit on the SM Higgs mass of $m_H > 65.2$ GeV [3]. The search for these particles and, if found, the exploration of their profile, will continue at LEP2 [4], the LHC [5], and future e^+e^- linear colliders [6].

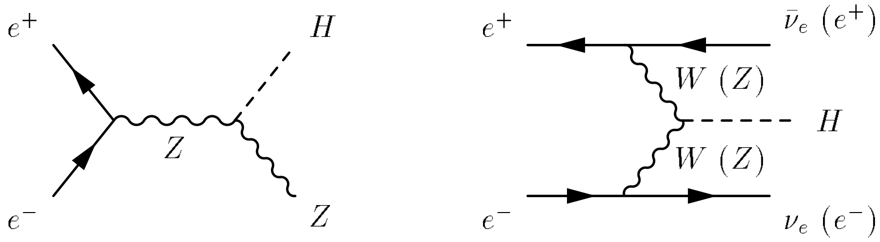

Figure 1: *Higgs-strahlung and vector boson fusion of (CP–even) Higgs bosons in e^+e^- collisions.*

In this note (see also [7]) we will focus on the production of scalar Higgs bosons in e^+e^- collisions. The main production mechanisms for these particles are Higgs-strahlung [8] and WW (ZZ) fusion [9–11] [supplemented in supersymmetric theories by associated scalar/pseudoscalar Higgs pair production]. In particular, we will present a comprehensive analysis of the interplay between the production mechanisms[1] (Fig.1)

$$
\begin{array}{lll}
\text{Higgs-strahlung}: & e^+e^- \to ZH \to \bar{\nu}\nu H & (e^+e^-H) \\
WW \text{ fusion} & : \; e^+e^- \to \bar{\nu}_e \nu_e H & \\
ZZ \text{ fusion} & : \; e^+e^- \to e^+e^- H &
\end{array}
\tag{1}
$$

For $\bar{\nu}_e\nu_e$ and e^+e^- decays of the Z bosons, the two production amplitudes interfere. It turns out that the interference term is positive for $\bar{\nu}_e\nu_e$ and negative for e^+e^- decays, respectively, in the cross-over region between the two mechanisms. The interference effect had been noticed earlier [9,13]; however, we improve on these calculations by deriving analytic results for the energy and polar angular distribution of the Higgs particle (E_H, θ) in the final states of $e^+e^- \to H +$neutrinos and $e^+e^- \to He^+e^-$. This representation can comfortably serve as input for Monte Carlo generators like PYTHIA/JETSET [14] and HZHA [15] which include the leading QED bremsstrahlung corrections and the important background processes.

2. Total cross sections. The cross section for the Higgs-strahlung process can be written in the following compact form:

$$
\sigma(e^+e^- \to ZH) = \frac{G_F^2 m_Z^4}{96\pi s} \left(v_e^2 + a_e^2\right) \lambda^{\frac{1}{2}} \frac{\lambda + 12 m_Z^2/s}{(1 - m_Z^2/s)^2}
\tag{2}
$$

where $\sqrt{s}$ is the center-of-mass energy, and $a_e = -1$, $v_e = -1 + 4\sin^2\theta_W$ are the Z charges of the electron; $\lambda = (1 - (m_H + m_Z)^2/s)\,(1 - (m_H - m_Z)^2/s)$ is the usual two-particle phase space function. So long as the non-zero width of the Z boson[2] is not taken into account, the cross section rises steeply at threshold $\sim (s - (m_H + m_Z)^2)^{1/2}$. After reaching a maximum [about 25 GeV above threshold in the LEP2 energy range], the cross section falls off at high energies, according to the scaling law $\sim g_W^4/s$ asymptotically. Thus, Higgs-strahlung is the dominant production process for moderate values of the energy. The cross section (2) for Higgs-strahlung is reduced by a factor $3 \times \mathrm{BR}_\nu = 20\%$ if the final state of Z decays is restricted to neutrino pairs.

The total cross section for the WW (ZZ) fusion of Higgs particles can be cast into a similarly compact form[3] [17]:

$$
\sigma = \frac{G_F^3 m_V^4}{64\sqrt{2}\,\pi^3} \int_{x_H}^1 dx \int_x^1 \frac{dy}{[1 + (y - x)/x_V]^2} \left[(v^2 + a^2)^2 f(x,y) + 4v^2 a^2 g(x,y)\right]
\tag{3}
$$

[1] We will concentrate first on the Standard Model (SM); the extension to the Minimal Supersymmetric Standard Model (MSSM) is trivial as will be demonstrated in the last section of this note.

[2] The results presented in this note are insensitive to non-zero width effects of the Higgs boson [16]. For SM Higgs masses below 100 GeV, Γ_H is at least three orders of magnitude smaller than Γ_Z; for larger Higgs masses, m_H can be reinterpreted as the effective invariant mass of the Higgs decay products.

[3] The variable x is the invariant mass squared of ν_e plus H, $(x - y)$ the 4-momentum transfer squared from e^+ to $\bar{\nu}_e$ (all momenta in units of the total energy).

where V denotes either W or Z, the charges are $v = a = \sqrt{2}$ ($v = v_e$ and $a = a_e$) for WW (ZZ) fusion, respectively, and

$$
\begin{aligned}
f(x,y) &= \left(\frac{2x}{y^3} - \frac{1+2x}{y^2} + \frac{2+x}{2y} - \frac{1}{2}\right)\left[\frac{z}{1+z} - \log(1+z)\right] + \frac{x}{y^3}\frac{z^2(1-y)}{1+z} \\
g(x,y) &= \left(-\frac{x}{y^2} + \frac{2+x}{2y} - \frac{1}{2}\right)\left[\frac{z}{1+z} - \log(1+z)\right]
\end{aligned}
$$

with $x_H = m_H^2/s$, $x_V = m_V^2/s$ and $z = y(x - x_H)/(xx_V)$. For moderate Higgs masses and energies, the cross section, being $\mathcal{O}(g_W^6)$, is suppressed with respect to Higgs-strahlung by the additional electroweak coupling. The smaller value of the Z-electron coupling suppresses the ZZ fusion process by an additional order of magnitude compared to WW fusion. At high energies, the WW fusion process becomes leading, nevertheless, since the size of the cross section is determined by the W mass, in contrast to the scale-invariant Higgs-strahlung process,

$$
\begin{aligned}
\sigma(e^+e^- \to \bar{\nu}_e\nu_e H) &\approx \frac{G_F^3 m_W^4}{4\sqrt{2}\,\pi^3}\left[\left(1 + \frac{m_H^2}{s}\right)\log\frac{s}{m_H^2} - 2\left(1 - \frac{m_H^2}{s}\right)\right] \\
&\to \frac{G_F^3 m_W^4}{4\sqrt{2}\,\pi^3}\log\frac{s}{m_H^2} \qquad (4)
\end{aligned}
$$

The cross section rises logarithmically at high energies, as to be anticipated for this t-channel exchange process.

3. Differential cross section and interference for WW fusion. The compact form (3) for the fusion cross section cannot be maintained once the interference term between vector boson fusion and Higgs-strahlung is included. Moreover, since in the case of WW fusion the integration variables x and y do not correspond to observable quantities, the formula is useful only for calculating the total cross section without experimental cuts. Nevertheless, similarly compact expressions can be derived in this general case by choosing the energy E_H and the polar angle θ of the Higgs particle as the basic variables in the e^+e^- c.m. frame. The overall cross section that will be observed experimentally for the process

$$e^+e^- \to H + \bar{\nu}\nu$$

receives contributions $3 \times \mathcal{G}_S$ from Higgs-strahlung with Z decays into three types of neutrinos, $\mathcal{G}_W$ from WW fusion, and $\mathcal{G}_I$ from the interference term between fusion and Higgs-strahlung for $\bar{\nu}_e\nu_e$ final states. We find[4] for energies $\sqrt{s}$ above the Z resonance:

$$\frac{d\sigma(H\bar{\nu}\nu)}{dE_H\, d\cos\theta} = \frac{G_F^3 m_Z^8 p}{\sqrt{2}\,\pi^3 s}\left(3\,\mathcal{G}_S + \mathcal{G}_I + \mathcal{G}_W\right) \qquad (5)$$

[4]The analytic result for $\mathcal{G}_W$ had first been obtained in Ref.[11].

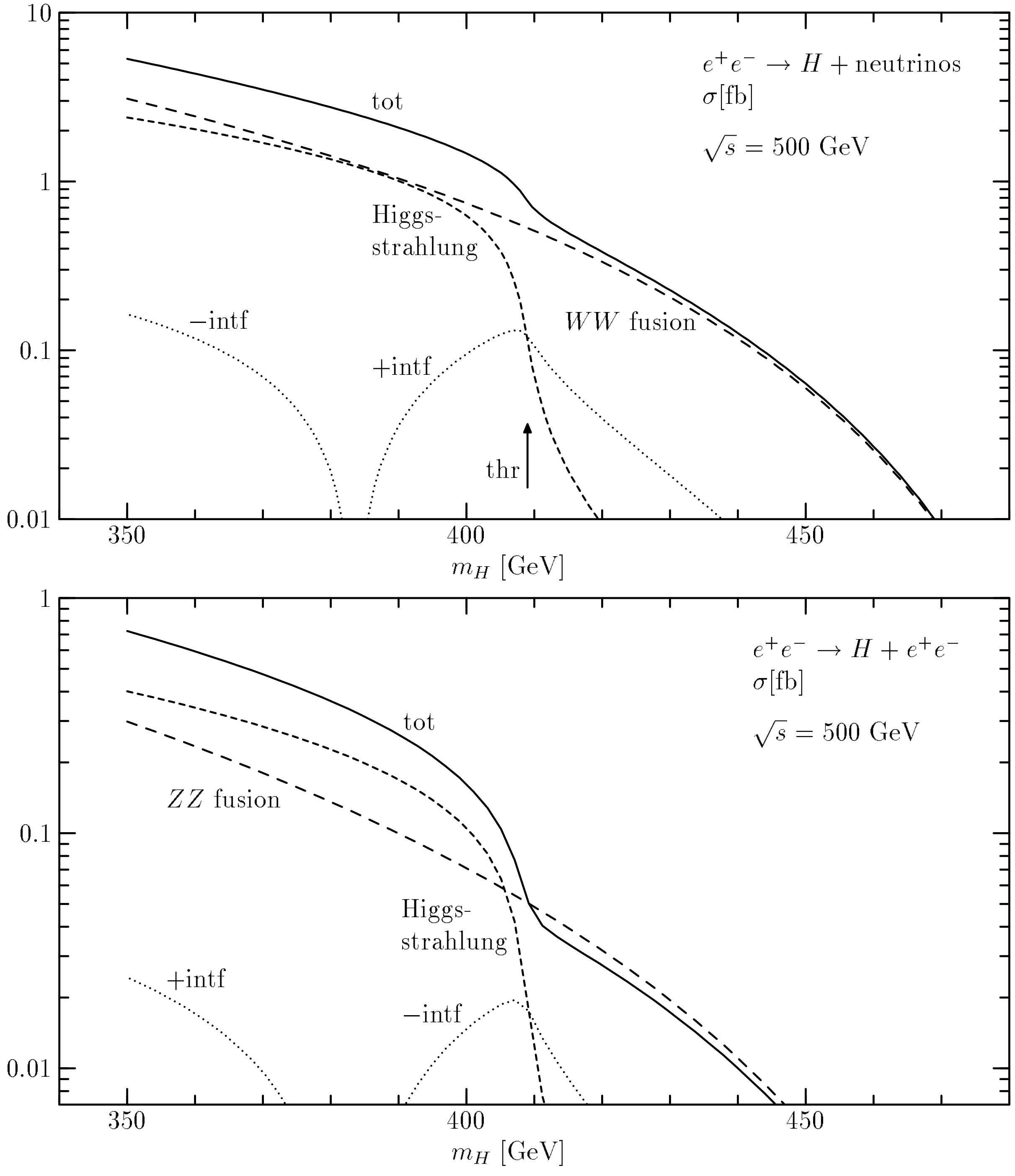

Figure 2: *Total cross sections for the processes* $e^+e^- \to H\bar{\nu}\nu$ *and* $e^+e^- \to He^+e^-$ *as a function of the Higgs mass. The cross sections are broken down to the three components Higgs-strahlung, vector boson fusion, and the interference term.* "thr" *denotes the maximum Higgs mass for on-shell* ZH *production,* "tot" *is the total cross section. In* $e^+e^- \to H\bar{\nu}\nu$ *(above) the interference term is negative for small Higgs masses, for large Higgs masses positive. In* $e^+e^- \to He^+e^-$ *(below), the interference term is of opposite sign.*

with

$$\mathcal{G}_S = \frac{v_e^2+a_e^2}{96}\,\frac{ss_\nu+s_1s_2}{(s-m_Z^2)^2\,[(s_\nu-m_Z^2)^2+m_Z^2\Gamma_Z^2]} \tag{6}$$

$$\begin{aligned}\mathcal{G}_I &= \frac{(v_e+a_e)\cos^4\theta_W}{8}\,\frac{s_\nu-m_Z^2}{(s-m_Z^2)\,[(s_\nu-m_Z^2)^2+m_Z^2\Gamma_Z^2]}\\ &\quad\times\left[2-(h_1+1)\log\frac{h_1+1}{h_1-1}-(h_2+1)\log\frac{h_2+1}{h_2-1}+(h_1+1)(h_2+1)\frac{\mathcal{L}}{\sqrt{r}}\right]\end{aligned} \tag{7}$$

$$\begin{aligned}\mathcal{G}_W &= \frac{\cos^8\theta_W}{s_1s_2r}\left\{(h_1+1)(h_2+1)\left[\frac{2}{h_1^2-1}+\frac{2}{h_2^2-1}-\frac{6s_\chi^2}{r}+\left(\frac{3t_1t_2}{r}-c_\chi\right)\frac{\mathcal{L}}{\sqrt{r}}\right]\right.\\ &\qquad\left.-\left[\frac{2t_1}{h_2-1}+\frac{2t_2}{h_1-1}+\left(t_1+t_2+s_\chi^2\right)\frac{\mathcal{L}}{\sqrt{r}}\right]\right\}\end{aligned} \tag{8}$$

The cross section is written explicitly in terms of the Higgs momentum $p=\sqrt{E_H^2-m_H^2}$, and the energy $\epsilon_\nu=\sqrt{s}-E_H$ and invariant mass squared $s_\nu=\epsilon_\nu^2-p^2$ of the neutrino pair. In addition, the following abbreviations have been adopted from Ref.[11],

$$\begin{aligned}
s_{1,2} &= \sqrt{s}(\epsilon_\nu \pm p\cos\theta) & t_{1,2} &= h_{1,2}+c_\chi h_{2,1}\\
h_{1,2} &= 1+2m_W^2/s_{1,2} & r &= h_1^2+h_2^2+2c_\chi h_1h_2-s_\chi^2\\
c_\chi &= 1-2ss_\nu/(s_1s_2) & \mathcal{L} &= \log\frac{h_1h_2+c_\chi+\sqrt{r}}{h_1h_2+c_\chi-\sqrt{r}}\\
s_\chi^2 &= 1-c_\chi^2 & &
\end{aligned}$$

To derive the total cross section $\sigma(e^+e^-\to H\bar\nu\nu)$, the differential cross section must be integrated over the region

$$-1<\cos\theta<1 \quad\text{and}\quad m_H<E_H<\frac{\sqrt{s}}{2}\left(1+\frac{m_H^2}{s}\right) \tag{9}$$

4. Differential cross section and interference for ZZ fusion. Similarly, the overall cross section for the process

$$e^+e^-\to H+e^+e^-$$

receives contributions $\mathcal{G}_S$ from Higgs-strahlung with Z decays into electron-positron pairs, $\mathcal{G}_Z$ from ZZ fusion, and $\mathcal{G}_I$ from the interference term between fusion and Higgs-strahlung:

$$\frac{d\sigma(He^+e^-)}{dE_H\,d\cos\theta}=\frac{G_F^3m_Z^8p}{\sqrt{2}\,\pi^3s}\,(\mathcal{G}_S+\mathcal{G}_I+\mathcal{G}_{Z1}+\mathcal{G}_{Z2}) \tag{10}$$

with

$$\mathcal{G}_S = \frac{(v_e^2+a_e^2)^2}{192}\,\frac{ss_e+s_1s_2}{(s-m_Z^2)^2\,[(s_e-m_Z^2)^2+m_Z^2\Gamma_Z^2]} \tag{11}$$

$$
\begin{aligned}
\mathcal{G}_I &= \frac{\left(v_e^2+a_e^2\right)^2+4v_e^2a_e^2}{64}\,\frac{s_e-m_Z^2}{(s-m_Z^2)\,[(s_e-m_Z^2)^2+m_Z^2\Gamma_Z^2]} \\
&\quad\times\left[2-(h_1+1)\log\frac{h_1+1}{h_1-1}-(h_2+1)\log\frac{h_2+1}{h_2-1}+\,(h_1+1)(h_2+1)\frac{\mathcal{L}}{\sqrt{r}}\right] \qquad (12)\\
\mathcal{G}_{Z1} &= \frac{\left(v_e^2+a_e^2\right)^2+4v_e^2a_e^2}{32\,s_1s_2r}\left\{(h_1+1)(h_2+1)\left[\frac{2}{h_1^2-1}+\frac{2}{h_2^2-1}-\frac{6s_\chi^2}{r}+\left(\frac{3t_1t_2}{r}-c_\chi\right)\frac{\mathcal{L}}{\sqrt{r}}\right]\right.\\
&\qquad\left.-\left[\frac{2t_1}{h_2-1}+\frac{2t_2}{h_1-1}+\left(t_1+t_2+s_\chi^2\right)\frac{\mathcal{L}}{\sqrt{r}}\right]\right\} \qquad (13)\\
\mathcal{G}_{Z2} &= \frac{\left(v_e^2-a_e^2\right)^2}{16\,s_1s_2r}(1-c_\chi)\left[\frac{2}{h_1^2-1}+\frac{2}{h_2^2-1}-\frac{6s_\chi^2}{r}+\left(\frac{3t_1t_2}{r}-c_\chi\right)\frac{\mathcal{L}}{\sqrt{r}}\right] \qquad (14)
\end{aligned}
$$

where the same abbreviations as in the formulae following Eq.(5), with the appropriate replacements $\nu \to e$ and $W \to Z$, have been used.

5. To interpret the results, we display the three components of the total cross sections $\sigma(e^+e^- \to H\bar{\nu}\nu)$ and $\sigma(e^+e^- \to He^+e^-)$ in Fig.2 for the linear collider energy $\sqrt{s} = 500$ GeV in the cross-over region.[5]

While the energy distribution of the Higgs particle peaks at $E_H \sim (s+m_H^2-m_Z^2)/2\sqrt{s}$ for Higgs-strahlung, it is nearly flat for WW fusion (Fig.3, left). Only with rising total energy the lower part of the Higgs spectrum becomes more pronounced. The angular distribution for Higgs-strahlung is almost isotropic at threshold while the standard $\sin^2\theta$ law is approached, in accordance with the equivalence principle, at asymptotic energies (Fig.3, right). The angular distribution peaks, by contrast, in the WW fusion process at $\theta \to 0$ and π for high energies as expected for t-channel exchange processes.

6. Polarized beams. At linear colliders the incoming electron and positron beams can be polarized longitudinally. Higgs-strahlung and WW fusion both require opposite helicities of the electrons and positrons. If $\sigma_{U,LR,RL}$ denote the cross sections in $e^+e^- \to H\bar{\nu}\nu$ for unpolarized electrons/positrons, left-handed electrons/right-handed positrons, and right-handed electrons/left-handed positrons, respectively, we can easily derive, in the notation of Eq.(5):

$$
\begin{aligned}
\sigma_U &\propto 3\,\mathcal{G}_S+\mathcal{G}_I+\mathcal{G}_W \qquad (15)\\
\sigma_{LR} &\propto 6\,\mathcal{G}_S+4\,\mathcal{G}_I+4\,\mathcal{G}_W \qquad (16)\\
\sigma_{RL} &\propto 6\,\mathcal{G}_S \qquad (17)
\end{aligned}
$$

The cross section for WW fusion of Higgs particles increases by a factor four, compared with unpolarized beams, if left-handed electrons and right-handed positrons are used. By using right-handed electrons, the WW fusion mechanism is switched off. [The interference term cannot be separated from the WW fusion cross section.]

---

[5]Note that Higgs-strahlung dominates WW fusion at 500 GeV for moderate Higgs masses only if the total ZH cross section is considered.

For the process $e^+e^- \to He^+e^-$, the pattern is slightly more complicated:

$$\sigma_U \propto \mathcal{G}_S + \mathcal{G}_I + \mathcal{G}_{Z1} + \mathcal{G}_{Z2} \tag{18}$$

$$\sigma_{LR} \propto 2\frac{(v_e+a_e)^2}{(v_e^2+a_e^2)}\mathcal{G}_S + 2\frac{(v_e+a_e)^4}{(v_e^2+a_e^2)^2+4v_e^2a_e^2}\left(\mathcal{G}_I + \mathcal{G}_{Z1}\right) \tag{19}$$

$$\sigma_{RL} \propto 2\frac{(v_e-a_e)^2}{(v_e^2+a_e^2)}\mathcal{G}_S + 2\frac{(v_e-a_e)^4}{(v_e^2+a_e^2)^2+4v_e^2a_e^2}\left(\mathcal{G}_I + \mathcal{G}_{Z1}\right) \tag{20}$$

$$\sigma_{LL} = \sigma_{RR} \propto 2\,\mathcal{G}_{Z2}. \tag{21}$$

However, since $v_e \ll a_e$, the difference between σ_{RL} and σ_{LR} is suppressed.

7. Supersymmetric CP-even Higgs bosons. It is trivial to transfer all these results from the Standard Model to the Minimal Supersymmetric Standard Model (MSSM). Since the couplings to Z/W gauge bosons in the MSSM are shared [20] by the CP-even light and heavy scalar Higgs bosons, h and H, respectively, only the overall normalization of the cross sections is modified with respect to the Standard Model:

$$\sigma(h)_{\mathrm{MSSM}} = \sin^2(\beta-\alpha) \times \sigma(H)_{\mathrm{SM}} \tag{22}$$

$$\sigma(H)_{\mathrm{MSSM}} = \cos^2(\beta-\alpha) \times \sigma(H)_{\mathrm{SM}} \tag{23}$$

Higgs-strahlung, vector boson fusion, and the interference term are affected in the same way. [The angle α is the mixing angle in the CP-even Higgs sector while the mixing angle β is determined by the ratio of the vacuum expectation values of the two neutral Higgs fields in the MSSM. A recent discussion of the size of the coefficients $\sin^2/\cos^2(\beta-\alpha)$ may be found in Ref.[21].]

References

[1] P.W. Higgs, Phys. Rev. Lett. 12 (1964) 132, and Phys. Rev. D145 (1966) 1156; F. Englert and R. Brout, Phys. Rev. Lett. 13 (1964) 321; G.S. Guralnik, C.R. Hagen, and T.W. Kibble, Phys. Rev. Lett. 13 (1964) 585.

[2] P. Fayet, Nucl. Phys. B90 (1975) 104.

[3] J.-F. Grivaz, Proceedings of the *International EPS Conference on High–Energy Physics*, Bruxelles 1995.

[4] M. Carena et al., *Higgs Physics*, in: Proceedings of the Workshop *Physics with LEP2*, eds. G. Altarelli and F. Zwirner, CERN 1995.

[5] G. Altarelli, Proceedings of the *ECFA LHC-Workshop*, eds. G. Jarlskog and D. Rein, Aachen 1990, CERN 90/10.

[6] Proceedings of the Workshop e^+e^- *Collisions at 500 GeV: The Physics Potential*, Munich–Annecy–Hamburg, ed. P.M. Zerwas, Reports DESY 92-123A,B; 93-123C.

[7] W. Kilian, M. Krämer, and P.M. Zerwas, Phys. Lett. B373 (1996) 135.

[8] J. Ellis, M.K. Gaillard, and D.V. Nanopoulos, Nucl. Phys. B106 (191976) 292; B.L. Ioffe and V.A. Khoze, Sov. J. Part. Nucl. 9 (1978) 50; B.W. Lee, C. Quigg, and H.B. Thacker, Phys. Rev. D16 (1977) 1519; J.D. Bjorken, Proc. *Summer Institute on Particle Physics*, SLAC Report 198 (1976).

[9] D.R.T. Jones and S.T. Petcov, Phys. Lett. B84 (1979) 440.

[10] R.N. Cahn and S. Dawson, Phys. Lett. B136 (1984) 96; G.L. Kane, W.W. Repko, and W.B. Rolnick, Phys. Lett. B148 (1984) 367; R.N. Cahn, Nucl. Phys. B255 (1985) 341; B.A. Kniehl, Z. Phys. C55 (1992) 605.

[11] G. Altarelli, B. Mele, and F. Pitolli, Nucl. Phys. B287 (1987) 205.

[12] S. Katsanevas et al., in preparation.

[13] E. Boos, M. Sachwitz, H. Schreiber, and S. Shichanin, Int. J. Mod. Phys. A10 (1995) 2067.

[14] T. Sjöstrand, *The PYTHIA 5.7 and JETSET 7.4 Manual*, LU–TP. 95/20 and CERN–TH 112/93, and Comput. Phys. Commun. 82 (1994) 74.

[15] P. Janot, *The HZHA Generator Program*, in preparation.

[16] A. Djouadi, M. Spira, and P.M. Zerwas, DESY 95-210 and Z. Phys. C in print.

[17] A. Djouadi, D. Haidt, B.A. Kniehl, B. Mele, and P.M. Zerwas, in Ref.[6].

[18] V.N. Baĭer, V.S. Fadin, and V.A. Khoze, Sov. Phys. JETP 23 (1966) 104.

[19] E. Boos et al., Report SNUTP–94–116.

[20] J.F. Gunion and H.E. Haber, Nucl. Phys. B272 (1986) 1; B278 (1986) 449; B307 (1988) 445; Erratum *ibid.* B402 (1993) 567; A. Djouadi, J. Kalinowski, and P.M. Zerwas, Z. Phys. C57 (1993) 569.

[21] A. Djouadi, J. Kalinowski, and P.M. Zerwas, DESY 95-211 and Z. Phys. C in print.

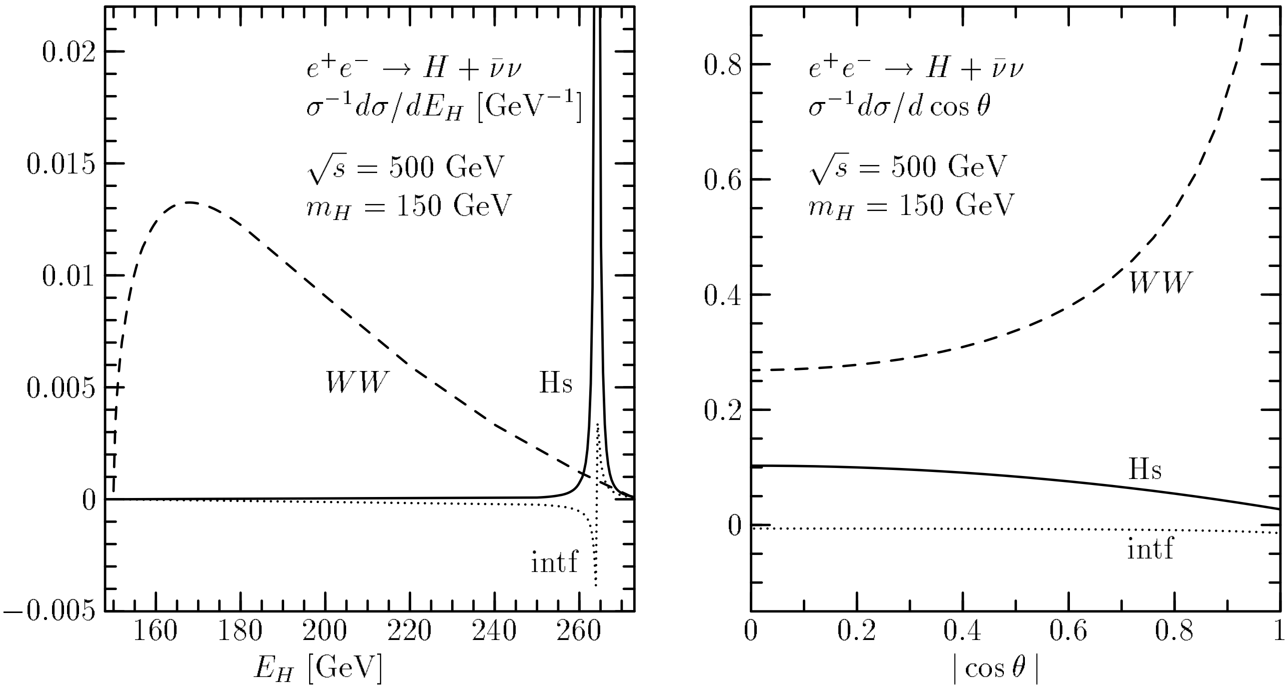

Figure 3: *Energy distribution (left) and angular distribution (right) of the Higgs bosons for the three components of the cross section [*Hs *= Higgs-strahlung;* WW *= fusion;* intf *= interference term]. The individual curves are normalized to the total cross section. The* Hs *peak extends up to maximal values of* 0.22 GeV^{-1}*. The total cross section is* 69.4 fb.